



Modelling of RC Beam-Column Exterior Joints for Cyclic Loadings

E. Grande¹, M. Imbimbo², A. Napoli³, R. Nitiffi²(✉), and R. Realfonzo³

¹ Department of Sustainability Engineering, University Guglielmo Marconi, Rome, Italy

² Department of Civil and Mechanical Engineering, University of Cassino and Southern Lazio, Cassino, Italy

riccardonitiffi@hotmail.it

³ Department of Civil Engineering, University of Salerno, Fisciano, Italy

Abstract. Recent and past seismic events have emphasized the key role of beam-column joints on the vulnerability of existing RC frame buildings. Indeed, damages and unexpected failure modes of these structural components in some cases resulted the main responsible of a poor seismic response of buildings. The lack of care by past standard codes for the design of beam-column joints and, moreover, the difficulties in modelling and simulating their complex behavior, are clearly highlighted by the available studies of literature, where the attention is mainly focused on the derivation of constitutive laws and numerical modelling approaches. The present paper concerns the numerical study of exterior RC beam-column joints. In particular, starting from the models available in literature, laws able to reproduce the monotonic and cyclic behavior are derived, implemented by using the simple scissors model and subsequently assessed toward experimental tests.

Keywords: RC beam – column joints · Experimental tests · Numerical analysis

1 Introduction

Severe damages and failures of existing reinforced concrete (RC) buildings observed during recent and past seismic events frequently involved exterior beam-column joints. Indeed, their configuration (unconfined joints) and deficiencies in terms of amount and details of steel reinforcement (lacks of stirrups and longitudinal steel bars without efficient anchorage ends) could make beam-column joints the weakest component of RC frames.

The literature contains a significant amount of studies concerning the experimental behavior of RC beam-column joints (De Risi et al. 2016, Realfonzo et al. 2014).

Other studies focus on the numerical modelling of the monotonic and cyclic response of RC beam-column joints (Alath and Kunnath 1995; Lowes and Altoontash 2003).

Nevertheless, the difficulties in reproducing the main phenomena affecting the monotonic and cyclic behavior of these elements and the importance of considering their role on the seismic response of existing buildings, make this topic of particular relevance and necessary to be further analysed.

Aim of this paper is to numerically simulate the monotonic and cyclic response of typical exterior beam–column joints without transverse reinforcements. To this purpose, constitutive laws obtained by combining some literature models are proposed. These are implemented into a simple model for beam-column joints where both the shear behavior and the possible occurrence of the slippage of longitudinal bars of beam from the joint are considered. The numerical analyses are carried out by using the open-source finite element platform OpenSees (McKenna et al. 2010).

The reliability of the obtained laws is assessed in the paper with reference to a set of seven experimental cases, representative of exterior joints without transverse reinforcements, collected from literature.

2 Shear Behavior of Exterior Joints: Literature Models

The experimental shear behavior of exterior beam–column joints can be described by the following main phenomena: a cracking process, the attainment of the peak strength, a subsequent process of strength degradation until the attainment of a residual shear strength value. This leads to adopt for its modelling a multi-linear shear stress-strain (τ - γ) constitutive law as that reported in Fig. 1. Then, the multi-linear law can be implemented into a macro-modelling approach available within the several commercial computer codes (McKenna et al. 2010) available nowadays, to perform numerical analyses.

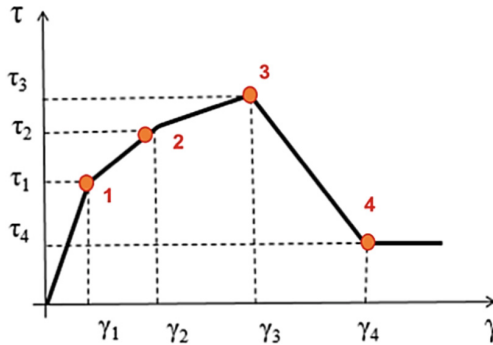


Fig. 1. Multilinear stress-strain relationship.

The multi-linear law is completely defined by four characteristic points in terms of stress ($\tau_1, \tau_2, \tau_3, \tau_4$) and strains ($\gamma_1, \gamma_2, \gamma_3, \gamma_4$).

In particular, regarding the evaluation of the shear strength τ_3 , (in the following indicated as τ_{max}) the following five models available in the literature are considered in the present paper.

The first model (*Model 1*), proposed by Kim and LaFave (2008), provides the following expression:

$$\tau_{max} = \alpha_t \beta_t \eta_t \lambda_t (JI)^{0.15} (BI)^{0.3} (f_c)^{0.75} \tag{1}$$

where: α_t is a coefficient depending on the joint configuration; β_t is a coefficient dependent on the level of the exterior joint's confinement; η_t is a coefficient related to the beam-column eccentricity; λ_t is a coefficient assumed equal to 1.31; f_c is the concrete compressive strength; JI represents the "joint transverse reinforcement index"; BI is the "beam reinforcement index".

The second model (*Model 2*) proposed by Vollum and Newman (1999), suggests the following expression:

$$\tau_{\max} = 0.642\beta \left[1 + 0.555 \left(2 - \frac{h_b}{h_c} \right) \right] \sqrt{f_c} \quad (2)$$

where: β is a coefficient depending on the configuration of the beam's longitudinal steel bar end inside the joint; h_b is the beam height; h_c is the column height.

The third model (*Model 3*), proposed by Ortiz (1993), provides:

$$\tau_{\max} = \frac{\sigma_d b_c w_j \cos \theta}{h_c b_c} \quad (3)$$

where: σ_d is the design compressive concrete strength estimated according to the CEB-FIP Model Code 90 (1993); b_c is the column width; b_b is the beam width; w_j is the strut width; θ is the angle between the strut and the longitudinal beam axis.

The fourth model (*Model 4*) is the one proposed by Hwang and Lee (1999) and suggests the following formula:

$$\tau_{\max} = \frac{D \cos \theta + F_h + F_v \cot \theta}{h_c b_c} \quad (4)$$

where: D is the compressive strength of the concrete strut component; F_h and F_v are respectively the horizontal and the vertical components of the tie member strength.

The last model (*Model 5*) by Jeon (2013) gives:

$$\tau_{\max} = 0.586(TB)^{0.774} (BI)^{0.495} (JP)^{1.25} (f_c)^{0.941} \quad (5)$$

where: TB coincides with the coefficient β_t of Eq. (1); JP corresponds to the coefficient α_t of Eq. (1).

A more detailed description of the five considered models can be found in Nitiffi et al. (2019).

Regarding the derivation of the other three values of the shear stresses (i.e. τ_1 , τ_2 , τ_4) and of the four shear strains (i.e. γ_1 , γ_2 , γ_3 , γ_4), other models are considered in the present paper.

In particular, for the shear stress τ_1 , the formula proposed by Uzumeri (1977) gives:

$$\tau_1 = 0.29 \sqrt{f_c} \sqrt{1 + 0.29 \frac{P}{A_j}} \quad (6)$$

where P is the column axial load and A_j is the effective joint area.

For the other parameters, the values proposed by De Risi et al. (2016), Celik and Ellingwood (2008), Shin and LaFave (2004) and Sharma et al. (2011) are considered

and summarized in Table 1. *Model A* indicates the model proposed by De Risi et al. (2016) and *Model D* that by Sharma et al. (2011); both these models propose a unique value for each of the above parameters. On the contrary the other two models propose a range of values for some of the parameters; *Models B1-B2* indicate the model by Celik and Ellingwood (2008) evaluated respectively for the minimum and maximum values of the range, and *Models C1-C2* indicate the one proposed by Shin and LaFave (2004) still at the minimum and maximum values of the ranges.

Table 1. Values derived from the accounted literature models

Model	τ_2/τ_{max}	τ_4/τ_{max}	γ_1	γ_2	γ_3	γ_4
A	0.85	0.43	0.0004	0.0017	0.0049	0.0441
B1	0.75	0.3	0.0001	0.002	0.01	0.03
B2	0.75	0.16	0.0013	0.01	0.03	0.1
C1	0.9	0.3	0.0005	0.002	0.01	0.03
C2	0.9	0.3	0.0005	0.01	0.03	0.05
D	0.9	0.24	0.0006	0.002	0.005	0.025

All the above models are combined in order to reproduce the shear response τ - γ of the panel zone. In particular, the shear strength τ_3 given by each of the *Models 1, 2, 3, 4, 5* is combined with the other parameters given by *Models A, B1, B2, C1, C2, D*. A total of 30 τ - γ relationships are, hence, obtained and summarized in Table 2. These laws are implemented in the numerical analyses, describing the monotonic shear behavior of RC beam-column joints, and presented in the following.

Table 2. Schematization of constitutive laws derived by combining the literature models

Model	A	B1	B2	C1	C2	D
1	1-A	1-B1	1-B2	1-C1	1-C2	1-D
2	2-A	2-B1	2-B2	2-C1	2-C2	2-D
3	3-A	3-B1	3-B2	3-C1	3-C2	3-D
4	4-A	4-B1	4-B2	4-C1	4-C2	4-D
5	5-A	5-B1	5-B2	5-C1	5-C2	5-D

3 Numerical Analyses

The definition of accurate constitutive laws reproducing the shear behavior of RC beam-column joints is an important preliminary step for performing numerical analyses based on macro-modelling approaches.

3.1 The Macro-Modelling Approach for RC Beam-Column Joints

In this study, the so-called “*scissors model*”, proposed by Alath and Kunnath (1995), is used. This model is composed of a rotational spring connecting a master node and a duplicated slave node located at the same position in the middle of the panel zone. Moreover, these nodes are connected to the beam and column members through rigid links.

In order to account for the contribution of the fixed-end-rotation due to the slip phenomenon of the longitudinal bars of the beam, an additional nonlinear rotational spring is introduced at the interface between the panel zone and the adjacent beam (Fig. 2).

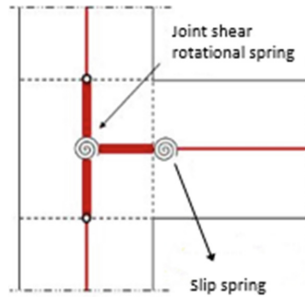


Fig. 2. Beam-column joint scissors model.

The numerical analyses are carried out by using the open-source finite element platform OpenSees (McKenna et al. 2010) where both the rotational springs have been modelled by the “*Pinching4 Uniaxial Material*” with a multi-linear law in terms of moment-rotation ($M-\theta$).

For what concern the joint shear spring, the ($M-\theta$) law is defined with the rotation of the spring θ_j assumed equal to the joint panel strain γ_j and the bending moment M_j given by:

$$M_j = \tau_j A \frac{1}{\frac{1-h_c/2L_b}{jd_b} - \frac{1}{2L_c}} \quad (7)$$

where: τ_j is the shear stress of the multilinear law; A is the joint cross-section area; h_c is the column height; L_b is the beam length; jd_b is the beam internal lever arm; L_c is the column length.

Regarding the spring modelling the bond slip behavior of the joint panel, the ($M-\theta$) law is that reported in Fig. 3 and defined as follows. Starting from the bond stress-slip

relationship reported in Model Code (2010), (see Fig. 3) the maximum moment M_3 is evaluated through the following formula:

$$M = f_{stm,tr} A_s j d_b \quad (8)$$

where A_s is the longitudinal reinforcement area of the beam and $f_{stm,tr}$ is the maximum tensile stress developed in the bar and transferred by bond. The latter parameter can be evaluated according to the Fédération Internationale (2010) as follows:

$$f_{stm,tr} = f_{stm} + 6 \left(\frac{l_b}{\phi} \right) p_{tr} \quad (9a)$$

where l_b and ϕ are the anchorage length of the longitudinal bar and its diameter, respectively, while f_{stm} and p_{tr} are given by:

$$f_{stm} = 54 \left(\frac{f_c}{25} \right)^{0.25} \left(\frac{l_b}{\phi} \right)^{0.55} \left(\frac{25}{\phi} \right)^{0.2} \left[\left(\frac{c_{\min}}{\phi} \right)^{0.25} \left(\frac{c_{\max}}{c_{\min}} \right)^{0.1} + k_m k_{tr} \right] \quad (9b)$$

$$p_{tr} = N / (b_c h_c) \quad (9c)$$

In Eqs. (9b) and (9c), c_{\min} and c_{\max} are geometrical parameters related to the concrete cover and the distance between adjacent bars respectively; k_m and k_{tr} are parameters related to eventual transverse reinforcements, evaluated as suggested by the Fédération Internationale (2010); N is the axial load on the column which is normalized with respect to the member cross-section area.

According to the mentioned Code, the following relationship should be satisfied:

$$f_{stm,tr} < 1.75 f_{st,0} + 0.8 \left(\frac{l_b}{p_{tr}} \right) < 8.0 \left(\frac{l_b}{\phi} \right) f_c^{0.5} \quad (9d)$$

where: $f_{st,0}$ is equal to f_{stm} in the particular condition of $c_{\min} = \emptyset$ and $c_{\max}/c_{\min} = 1$.

The moment M_2 and M_4 , instead, are assumed respectively equal to $0.75M_3$ and $0.40M_3$, according to De Risi et al. (2016).

The rigid rotation θ_s of the joint panel due to the slip is obtained from the proposal by Otani and Sozen (1972) (Eq. 10), neglecting the slip of the bar in compression:

$$\theta_s = \frac{slip}{d - d'} \quad (10)$$

where $(d-d')$ is the distance between the longitudinal reinforcements in tension and compression.

In particular, the slip values are deduced from the Fédération Internationale (2010) in the case of pull-out failure: s_2 is assumed equal to 1.8 mm, corresponding to the attainment of the bond strength; s_3 is assumed equal to 3.6 mm, corresponding to the beginning of the bond strength degradation; s_4 is assumed equal to 12 mm.

Finally, the value of M_1 and the corresponding slip s_1 , have been directly obtained from the intersection of the first branch (corresponding to the rigid un-cracked phase) and the third branch of the adopted law. Indeed, since frame elements with a nonlinear

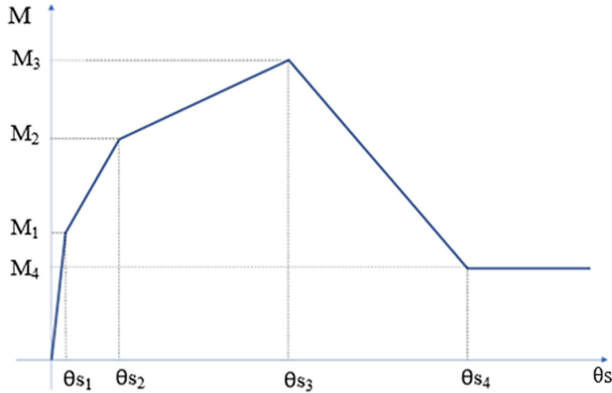


Fig. 3. Multilinear moment-rotation relationship for the bond-slip behavior.

behavior are considered in the modelling approach employed by the authors, the cracking effect is directly introduced at the beam section level.

The aim of the numerical analyses here presented is to assess the reliability of the obtained law in reproducing the monotonic experimental behavior of beam-column joints. Then, a set of specimens available in literature, representative of typical exterior RC beam – column joints and subjected to cyclic load histories have been considered.

In particular, the accounted set of experimental cases concerns the tests carried out by Realfonzo et al. (2014), Pantelides et al. (2002), Clyde et al. (2000), De Risi et al. (2016), Del Vecchio et al. (2014).

Table 3 summarizes the main informations on these case studies, where b_b and h_b are the width and the depth of the beam member, $A_{s,b}$ is the beam longitudinal reinforcement area, whereas the other symbols were already defined earlier.

For each case, monotonic analyses have been performed by accounting for the 30 $\tau - \gamma$ constitutive laws. The obtained results in terms of applied force vs. drift (the latter corresponding to the ratio between the displacement at the end of the beam and the beam length) are compared with the envelope of the experimental hysteretic cycles.

The relative error between the experimental and numerical forces is calculated up to the conventional value of 75% of the maximum experimental strength (both in the positive and negative direction of loading) through the following formula:

$$Err = \frac{\sum_{i=1}^n E_i}{n}; E_i = \frac{|F_{exp,i} - F_{num,i}|}{F_{exp,i}} 100 \quad (11)$$

where: $F_{exp,i}$ and $F_{num,i}$ are the i -th experimental force and the corresponding numerical force respectively.

Tables 4a and 4b provide the percent error values for the positive branch and negative branch of the envelope curve, respectively. As noted, the models furnishing the lowest error vary among the accounted experimental tests. Indeed:

- test J05: the lowest error values, equal to 9% and 6%, are provided by the *model 5CI*;
- test J01: the lowest error values, equal to 15% and 14%, are provided by the *model 1CI*;

Table 3. Main geometric and mechanical properties of the experimental database.

ID		b_c [mm]	h_c [mm]	b_b [mm]	h_b [mm]	$A_{s,b}$ [mm ²]	L_c [mm]	L_b [mm]	f_c [MPa]
[1]	J01	300	300	300	400	1885	2600	1580	14
	J05	300	300	300	400	2513	2600	1580	14
[2]	TU3	406	406	406	406	4927	3200	1689	34
	TU1	406	406	406	406	4927	3200	1689	33.1
[3]	#4	457	305	305	406	4927	2570	1498	41
[4]	T#1	300	300	300	500	2513	3400	1800	28.8
[5]	TC3	300	300	300	500	1608	3400	1800	16.3

[1] Realfonzo et al. (2014); [2] Pantelides et al. (2014); [3] Clyde et al. (2000); [4] De Risi et al. (2016); [5] Del Vecchio et al. (2014).

- test TU3: the lowest error values, equal to 17% and 12%, are provided by the *model 5A*;
- test TU1: the lowest error value, equal to 19%, is provided by the *model 5A*; in this case, the errors for the negative branch are related to the bond-slip mechanism and not accounted in this study;
- test #4: the lowest error values equal, to 11% and 7%, are provided by the *model 5A*;
- test T#1: the lowest error values, equal to 17% and 34%, are provided by the *model 1A*;
- test T_C3: the lowest error values, equal to 15% and 14%, are provided by the *model 4A*.

It must be highlighted that the *models B2* and *C2* are not taken into account in the assessment of the percentage errors, due to relevant drift excursions for the current experimental case studies.

The comparison between the numerical curves and experimental monotonic envelopes considering the models furnishing the lowest error is shown in Figs. 4, 5 and 6.

It is possible to observe a good agreement between numerical and experimental results, even in terms of failure mode prediction; besides the joints affected by the shear failure of the panel zone, the anchorage failure of the specimen TU1 (Pantelides et al. 2002) is also captured.

Table 4a. Mean absolute percentage errors [%] for the monotonic envelopes (positive branch)

model	J05	J01	TU3	TU1	#4	T#1	T_C3
1A	10	17	18	24	25	17	18
1B1	14	17	27	34	27	25	26
1B2	n.a	n.a	n.a	n.a	n.a	n.a	n.a
1C1	13	15	28	32	25	28	25
1C2	n.a	n.a	n.a	n.a	n.a	n.a	n.a
1D	19	19	42	41	32	37	35
2A	24	53	29	26	19	42	6
2B1	15	47	27	29	21	43	12
2B2	n.a	n.a	n.a	n.a	n.a	n.a	n.a
2C1	21	51	28	30	19	39	8
2C2	n.a	n.a	n.a	n.a	n.a	n.a	n.a
2D	20	35	35	36	24	47	23
3A	19	55	17	22	28	22	26
3B1	14	48	26	32	29	27	35
3B2	n.a	n.a	n.a	n.a	n.a	n.a	n.a
3C1	15	53	27	30	27	30	37
3C2	n.a	n.a	n.a	n.a	n.a	n.a	n.a
3D	21	36	41	40	33	37	45
4A	19	53	15	21	21	16	15
4B1	14	47	25	30	23	25	22
4B2	n.a	n.a	n.a	n.a	n.a	n.a	n.a
4C1	17	51	26	29	21	29	21
4C2	n.a	n.a	n.a	n.a	n.a	n.a	n.a
4D	20	35	39	39	27	37	33
5A	14	27	17	19	11	25	16
5B1	13	22	25	27	16	28	23
5B2	n.a	n.a	n.a	n.a	n.a	n.a	n.a
5C1	9	23	25	28	14	30	22
5C2	n.a	n.a	n.a	n.a	n.a	n.a	n.a
5D	22	18	37	37	13	37	33

n.a.: value not accounted

Table 4b. Mean absolute percentage errors [%] for the monotonic envelopes (negative branch)

model	J05	J01	TU3	TU1	#4	T#1	T_C3
1A	10	14	19	19*	15	34	22
1B1	14	16	29	19*	19	36	28
1B2	n.a	n.a	n.a	28*	n.a	n.a	n.a
1C1	11	14	29	19*	15	35	27
1C2	n.a	n.a	n.a	25*	n.a	n.a	n.a
1D	21	18	39	19*	22	42	36
2A	18	36	21	19*	9	60	25
2B1	10	28	31	19*	14	56	17
2B2	n.a	n.a	n.a	25*	n.a	n.a	n.a
2C1	15	36	28	19*	10	55	18
2C2	16	n.a	n.a	22*	n.a	n.a	n.a
2D	16	23	21	19*	15	47	24
3A	14	37	17	19*	17	41	18
3B1	13	30	26	19*	20	39	27
3B2	n.a	n.a	n.a	28*	n.a	n.a	n.a
3C1	11	36	27	19*	17	38	27
3C2	n.a	n.a	n.a	26*	n.a	n.a	n.a
3D	15	24	38	19*	24	42	37
4A	14	36	14	19*	11	32	14
4B1	9	29	24	19*	15	36	15
4B2	n.a	n.a	n.a	27*	n.a	n.a	n.a
4C1	12	36	26	19*	11	34	16
4C2	n.a	n.a	n.a	24*	n.a	n.a	n.a
4D	16	23	36	19*	17	43	29
5A	9	18	12	19*	7	43	22
5B1	11	17	23	19*	13	41	28
5B2	n.a	n.a	n.a	26*	n.a	n.a	n.a
5C1	6	16	24	19*	9	43	31
5C2	n.a	n.a	n.a	23*	n.a	n.a	n.a
5D	15	17	32	19*	5	42	37

n.a.: value not accounted; *: value related to the bond-slip spring

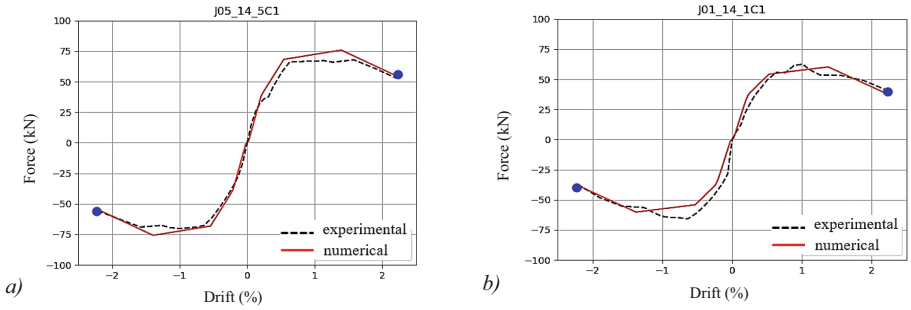


Fig. 4. Comparison between numerical curves and experimental envelope: test J05 (a) and J01 (b) by Realfonzo et al. (2014).

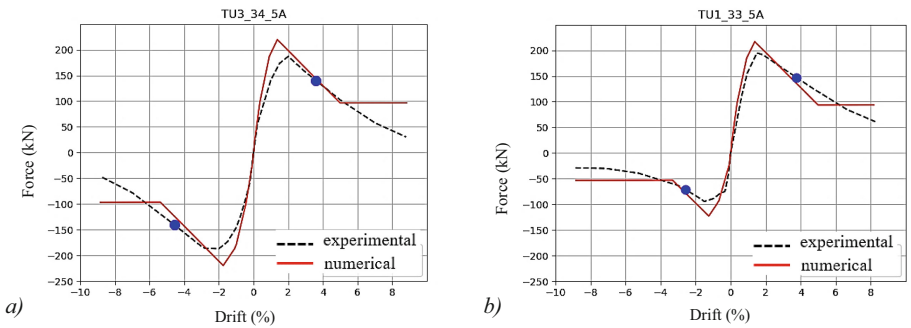


Fig. 5. Comparison between numerical curves and experimental envelope: test TU3 (a) and TU1 (b) by Pantelides et al. (2002).

4 Assessment of the Joint Shear Strength

The monotonic simulations in Figs. 4, 5 and 6 highlight the strong correlation between the numerical evaluation of the global shear strength of joints and the correct estimate of the shear stress τ_{max} . Preliminary considerations are here carried out by comparing the values of $\tau_{max,num}$ obtained from the analyzed *Models 1 to 5* with the experimental value of shear strength ($\tau_{max,exp}$) obtained from the equilibrium of the forces acting on the joint panel:

$$\tau_{max,exp} = \frac{T_b - V_{col}}{A_j} \quad (12)$$

where T_b is the tensile force acting in the longitudinal bars of the beam, V_{col} is the column shear force, A_j the cross-section area of the joint.

The scatter between the numerical and the experimental strength is calculated through the mean absolute percentage error as follows:

$$Err = \frac{\sum_{i=1}^n E_i}{n} =; E_i = \frac{|\tau_{max,exp,i} - \tau_{max,num,i}|}{\tau_{max,exp,i}} 100 \quad (13)$$

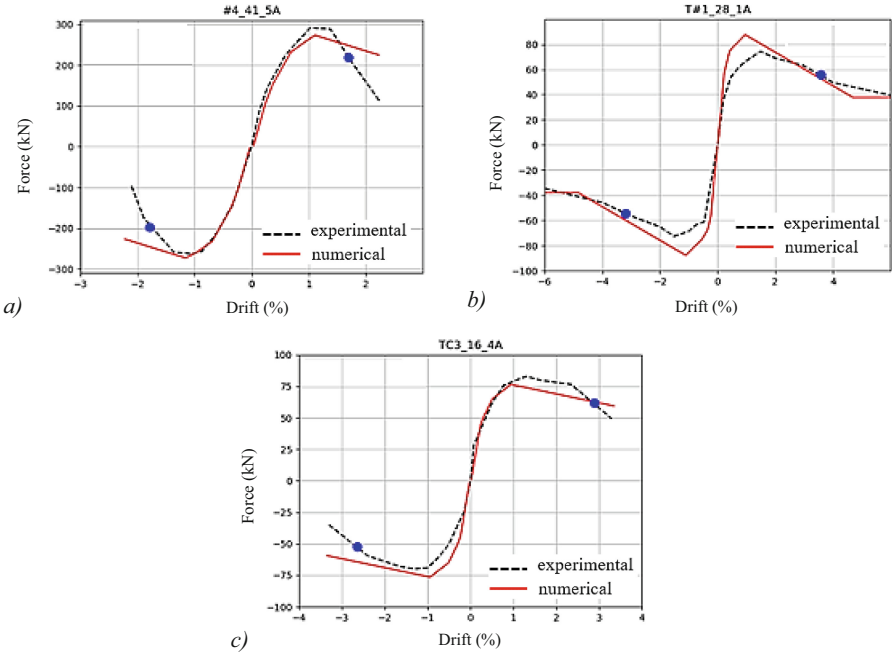


Fig. 6. Comparison between numerical curves and experimental envelope: specimens tested by (a) Clyde et al. (2000); (b) De Risi et al. (2016); (c) Del Vecchio et al. (2014).

where $\tau_{max,exp,i}$ and $\tau_{max,num,i}$ are the i -th experimental and the i -th numerical shear strength, respectively.

The bar charts in Figs. 7a and b depict the errors for both the positive (“+”) and negative (“-”) direction of loading in terms of the maximum shear strength estimated according to the considered five models. An exception is represented by the specimen TU1 (Pantelides et al. 2002) for which only the errors in the push (positive) direction were calculated since an anchorage failure due to loss of bond was experienced in the pull (negative) direction.

The bar chart in Fig. 8, instead, shows the mean error in the estimate of τ_{max} computed by the models on all the considered tests and considering both the positive and negative directions together; the errors bars show the positive and negative deviation of the error from the mean value computed for each model.

From these graphs it can be noted that the accuracy of the all models is rather variable with the considered test. Overall, *Model 1* (Kim and LaFave 2008) and *Model 5* (Jeon 2013) seem to provide values of shear strength closer to the those emerged from experimental tests, since the mean errors amount to 13.6% and 14.6%, respectively (see Fig. 8).

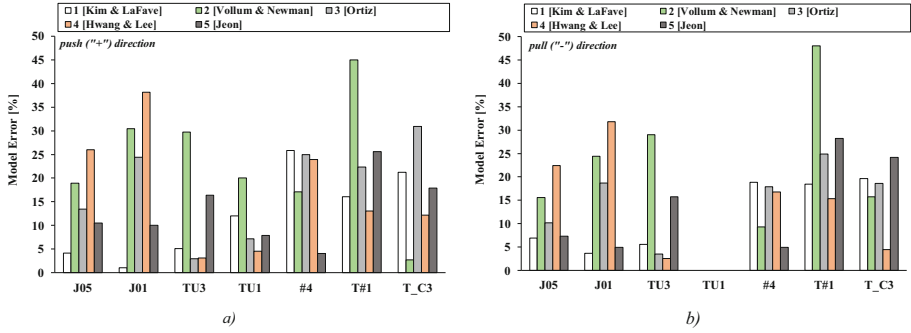


Fig. 7. Model errors in terms of τ_{\max} by varying the considered experimental test: push direction (a); pull direction (b).

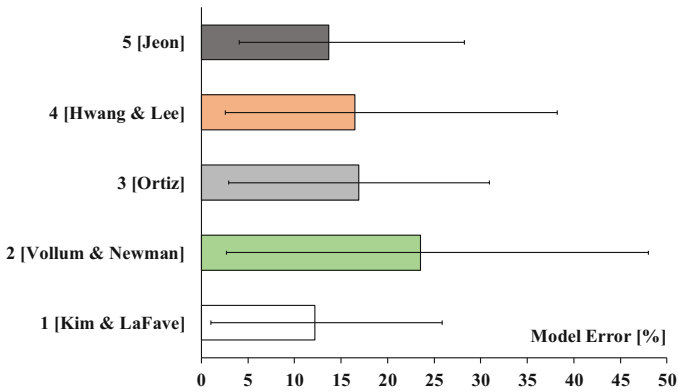


Fig. 8. Model errors in terms of τ_{\max} on all the tests.

5 Cyclic Response

The modelling of the cyclic behavior represents another key aspect in the study of the seismic response of the RC beam-column joints with a greater complexity with the respect to the monotonic behavior.

The constitutive laws obtained in the previous sections represent a valuable basis for carrying out cyclic analyses. Then, implementing the macro-modelling approach described in Sect. 2 and picking the laws providing the lowest value of the errors, cyclic analyses have been performed.

Regarding the shear behavior of the panel joint a calibration procedure has been done for the material model *Pinching 4*. To this purpose, for all the analyzed specimens, the parameters obtained from a calibration procedure carried out by Nitiffi et al. (2019) on the specimen J05 (Realfonzo et al. 2014) have been considered.

The results of these preliminary analyses in terms of cyclic behavior are compared with the experimental response in Fig. 9. The graphs show a general good agreement between experimental and numerical cyclic curves.

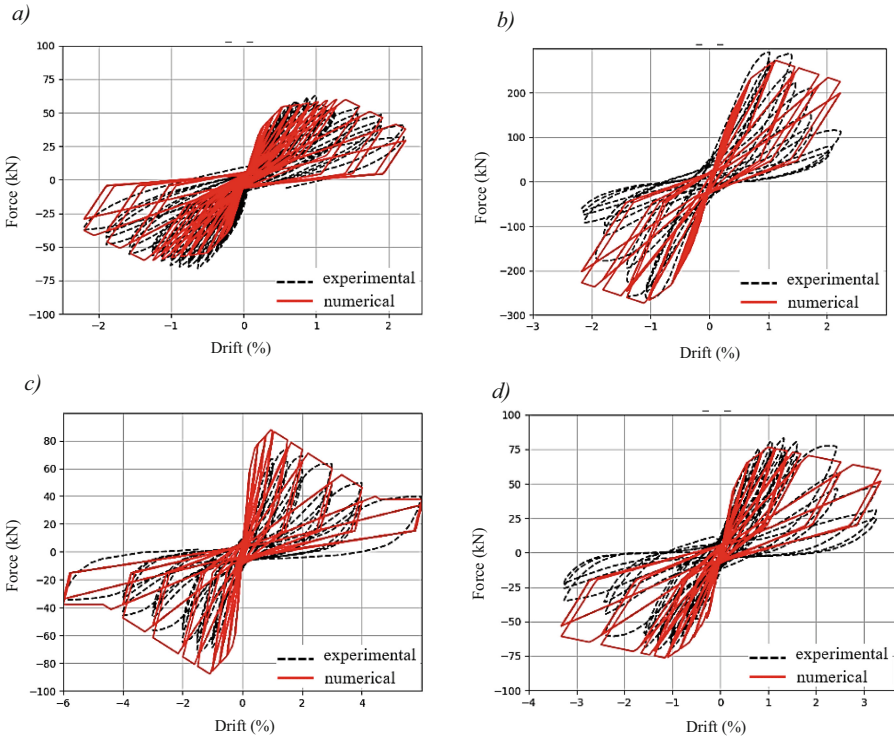


Fig. 9. Comparison between numerical and experimental cyclic curves: (a) test J01 by Realfonzo et al. (2014); (b) test #4 by Clyde et al. (2000); (c) test T#1 by De Risi et al. (2016); (d) test TC3 by Del Vecchio et al. (2014).

6 Conclusions

In this study, a procedure has been presented for the calibration of constitutive laws to employ into numerical models for the study of the monotonic and cyclic response of beam-column joints. In particular, 30 laws have been obtained by opportunely combining some models available in literature.

The 30 laws have been implemented in a simple model where the behavior of joint is schematized throughout two rotational springs in series: one reproducing the shear behavior and the other the bond-slip behavior.

Numerical analyses, both monotonic and cyclic, have been then performed by selecting seven experimental cases from the literature. The monotonic analyses have allowed to identify the combinations of models which better simulate the experimental response of the specimens. Furthermore, the better laws have been subsequently used for performing preliminary cyclic analyses. The obtained results have underlined a good ability of the derived laws in reproducing both the monotonic and cyclic response of beam-column joints.

Further developments are needed to assess the proposed model for a wider experimental database, also including different joint configurations and structural details.

Acknowledgements. The financial support by ReLUIIS (Network of the Italian University Laboratories for Seismic Engineering – Italian Department of Civil Protection) is gratefully acknowledged (Executive Project 2019–21 - WP14/WP2 CARTIS).

References

- Alath, S., Kunnath, S.K.: Modeling inelastic shear deformations in RC beam–column joints. In: Engineering Mechanics Proceedings of 10th Conference, vol. 2, pp. 822–825. ASCE, New York (1995)
- Comite, Euro-International Du, Beton: CEB-FIP Model Code 1990. Thomas Telford Services, London (1993)
- Celik, O.C., Ellingwood, B.R.: Modeling beam column joints in fragility assessment of gravity load designed reinforced concrete frames. *J. Earthquake Eng.* **12**, 357–381 (2008)
- Clyde, C., Pantelides, C.P., Reavely, L.D.: Performance-Based evaluation of exterior reinforced concrete building joints for seismic excitation. PEER report 2000/05, Berkeley, CA, USA, Pacific Earthquake Engineering Research Center, University of California (2000)
- De Risi, M.T., Ricci, P., Verderame, G.M.: Modelling exterior unreinforced beam – column joints in seismic analysis of non – ductile RC frames. *Earthquake Eng. Struct. Dynam.* **46**(6), 899–923 (2016)
- Del Vecchio, C., Di Ludovico, M., Balsamo, A., Prota, A., Manfredi, G., Dolce, M.: Experimental investigation of exterior RC beam-column joints retrofitted with FRP systems. *J. Compos. Constr.* **18**(04014002), 1–13 (2014)
- Fédération Internationale du Béton fib/International Federation for Structural Concrete. In: Fib Model Code for Concrete Structures. Ernst & Sohn, Hoboken, New Jersey (2010)
- Hwang, S., Lee, H.: Analytical model for predicting shear strengths of exterior reinforced concrete beam-column joints for seismic resistance. *ACI Struct. J.* **96**(5), 846–857 (1999)
- Jeon, J.S.: Aftershock vulnerability assessment of damaged reinforced concrete buildings in California. Ph.D. Thesis, School of Civil and Environmental Engineering, Georgia Institute of Technology, GA, USA (2013)
- Kim, J., LaFave, J.M.: Joint shear behavior prediction in RC beam-column connections subjected to seismic lateral loading. In: Proceedings of the 14th World Conference on Earthquake Engineering, Beijing, China, 12–17 October 2008 (2008)
- McKenna, F., Fenves, G.L., Scott, M.H.: OpenSees: Open System for Earthquake Engineering Simulation. Pacific Earthquake Engineering Research Center. University of California, Berkeley, CA, USA (2010)
- Nitiffi, R., Grande, E., Imbimbo, M., Napoli, A., Realfonzo, R.: Exterior RC beam-column joints: experimental outcomes and modeling issues. In: Proceedings of the XVIII Anidis Congress “L’Ingegneria Sismica in Italia”, Ascoli Piceno, Italy, 15–19 September 2019 (2019)
- Ortiz, I.R.: Strut-and-Tie Modeling of Reinforced Concrete Short Beams and Beam-Column Joints. Ph.D. Thesis, London, United Kingdom: University of Westminster (1993)
- Otani, S., Sozen, M.A.: Behavior of multistory reinforced concrete frames during earthquakes. A Report on a Research Project Sponsored by The National Science Foundation Research Grant Gi 30760x, University of Illinois, Engineering Experiment Station (1972)
- Lowe, L.N., Altoontash, A.: Modeling reinforced-concrete beam-column joints subjected to cyclic loading. *ASCE J. Struct. Eng.* **129**(12), 1686–1697 (2003)
- Pantelides, C.P., Hansen, J., Nadauld, J., Reavely, L.D.: Assessment of reinforced concrete building exterior joints with substandard details. PEER Report 2002/18, Berkeley, CA, USA, Pacific Earthquake Engineering Research Center, University of California (2002)

- Realfonzo, R., Napoli, A., Ruiz Pinilla, J.G.: Cyclic behavior of RC beam-column joints strengthened with FRP systems. *Constr. Build. Mater.* **54**, 282–297 (2014)
- Sharma, A., Eligehausen, R., Reddy, G.R.: A new model to simulate joint shear behavior of poorly detailed beam–column connections in RC structures under seismic loads, part I: exterior joints. *Eng. Struct.* **33**(3), 1034–1051 (2011)
- Shin, M., LaFave, J.M.: Testing and modelling for cyclic joint shear deformations in RC beam–column connections. In: *Proceedings of the Thirteenth World Conference on Earthquake Engineering*, Vancouver, B.C., Canada, 1–6 August 2004 (2004)
- Uzumeri, S.M.: Strength and ductility of cast-in-place beam-column joints, American concrete institute annual convention. *Symp. Reinforced Concr. Struct. Seismic Zones* **53**, 293–350 (1977)
- Vollum, R.L., Newman, J.B.: Strut and tie models for analysis/design of external beam-column joints. *Mag. Concr. Res.* **51**(6), 415–425 (1999)